

Mechanistic study of secondary organic aerosol components formed from nucleophilic addition reactions of methacrylic acid epoxide

A. W. Birdsall,* C. R. Miner, L. E. Mael, and M. J. Elrod

Department of Chemistry and Biochemistry, Oberlin College, Oberlin, Ohio, USA

Correspondence to: M. J. Elrod (mjelrod@oberlin.edu)

*Current affiliation: Department of Chemistry, University of Wisconsin-Madison, Madison, Wisconsin, USA

Abstract

Recently, methacrylic acid epoxide (MAE) has been proposed as a precursor to an important class of isoprene-derived compounds found in secondary organic aerosol (SOA): 2-methylglyceric acid (2-MG) and a set of oligomers, nitric acid esters and sulfuric acid esters related to 2-MG. However, the specific chemical mechanisms by which MAE could form these compounds have not been previously studied with experimental methods. In order to determine the relevance of these processes to atmospheric aerosol, MAE and 2-MG have been synthesized and a series of bulk solution-phase experiments aimed at studying the reactivity of MAE using nuclear magnetic resonance (NMR) spectroscopy have been performed. The present results indicate that the acid-catalyzed MAE reaction is more than 600 times slower than a similar reaction of an important isoprene-derived epoxide, but is still expected to be kinetically feasible in the atmosphere on more acidic SOA. The specific mechanism by which MAE leads to oligomers was identified, and the reactions of MAE with a number of atmospherically relevant nucleophiles were also investigated. Because the nucleophilic strengths of water, sulfate, alcohols (including 2-MG), and acids (including MAE and 2-MG) in their reactions with MAE were found to be of a similar magnitude, it is expected that a diverse variety of MAE + nucleophile product species may be formed on ambient SOA. Thus, the results indicate that epoxide chain reaction oligomerization will be limited by the presence of high concentrations of non-epoxide nucleophiles (such as water); this finding is consistent with previous environmental chamber investigations of the relative humidity-dependence of 2-MG-derived oligomerization processes and suggests that extensive

1 oligomerization may not be likely on ambient SOA because of other competitive MAE
2 reaction mechanisms.

3

4 **1 Introduction**

5 Due to isoprene's significant contribution to global secondary organic aerosol (SOA) (Carlton
6 et al., 2009; Hallquist et al., 2009), the atmospheric chemical mechanisms by which this
7 volatile substance is converted into aerosol phase components have recently received intense
8 scrutiny. Previous studies using environmental chamber experiments have shown that
9 isoprene-derived SOA can be formed through an oxidation pathway that begins with
10 methacrolein, a first-generation product of isoprene oxidation, and results in the formation of
11 2-methylglyceric acid (2-MG), a compound that has been observed in laboratory-generated
12 and ambient atmospheric SOA (Surratt et al., 2006; Jaoui et al., 2008; Edney et al., 2005;
13 Szmigielski et al., 2007; Zhang et al., 2011). Further environmental chamber studies have
14 established that methacryloylperoxynitrate (MPAN) is a second-generation oxidation product
15 in this pathway (Surratt et al., 2010).

16

17 In addition to 2-MG itself, related compounds have also been observed on SOA. In
18 environmental chamber experiments, oligomers, nitric acid esters, and sulfuric acid esters
19 structurally related to 2-MG have been characterized using a variety of chromatographic and
20 mass spectroscopic techniques (Chan et al., 2010a; Surratt et al., 2007; Szmigielski et al.,
21 2007; Hatch et al., 2011a; Gómez-González et al., 2008; Zhang et al., 2011). In one case, the
22 observation of a dimer containing two 2-MG subunits connected via an ester linkage in
23 ambient aerosol has been reported (Jaoui et al., 2008). These species are of particular interest
24 in understanding SOA composition because they possess volatilities even lower than that of
25 2-MG, due to increased molecular weights and/or the presence of highly polar nitrate and
26 sulfate groups.

27

28 Recent atmospheric chamber experiments suggest that water content (i.e., relative humidity
29 (RH)) plays a large role in determining the extent of oligomerization of species containing 2-
30 MG subunits. Under conditions of very low water content (RH<2%), the photooxidation of
31 isoprene was observed to lead to 2-MG-derived oligoesters up to 8 units in length (Nguyen et
32 al., 2011). On the other hand, a 69% reduction in 2-MG oligomer formation was observed

1 under high water content (RH=90%) conditions. Similarly, a second investigation of isoprene-
2 derived SOA found that the extent of 2-MG-derived oligomerization decreased by almost a
3 factor of 4 as the water content was increased from 13% RH to 88% RH (Zhang et al., 2011).
4 A third study of methacrolein-derived SOA determined that 2-MG-derived oligomerization
5 was extensive at <10% RH, with up to five 2-MG units in the oligomers (Chan et al., 2010a).

6

7 The mechanisms by which sulfate esters, nitrate esters, and oligoesters containing 2-MG are
8 formed, and the conditions necessary for efficient formation, are currently unknown. One
9 possible source of these compounds is via acid-catalyzed reactions of 2-MG itself. In
10 particular, a Fischer esterification mechanism would allow for oligomeric chains of 2-MG to
11 be formed or for nitrate and sulfate ester formation in the presence of those inorganic ions.
12 However, previous kinetics measurements suggest that, under the typical range of aerosol
13 conditions, Fischer esterification of 2-MG proceeds too slowly to account for the extent of
14 oligomer formation observed in atmospheric chamber experiments (Birdsall et al., 2013).

15

16 Recent atmospheric chamber studies and field observations have demonstrated that an
17 epoxide species, methacrylic acid epoxide (MAE), may be, via hydrolysis reaction, the
18 precursor to 2-MG formation (Lin et al., 2013). Therefore, it is also quite possible that the
19 various classes of esters containing 2-MG units identified in atmospheric chamber
20 experiments may also be products of MAE reactions, rather than of reactions solely involving
21 2-MG. Indeed, in an analogous situation, laboratory studies of isoprene-derived SOA-phase
22 chemistry (Lin et al., 2012; Surratt et al., 2010; Darer et al., 2011; Hu et al., 2011; Cole-
23 Filipiak et al., 2010) and field observations of SOA (Hatch et al., 2011b; Surratt et al., 2010;
24 Chan et al., 2010b) for isoprene-dominated situations have uncovered evidence that many of
25 the individual isoprene backbone-retaining chemical species observed are the result of the
26 SOA-phase reactions of isoprene epoxydiols (IEPOX) (Paulot et al., 2009). Therefore, it is of
27 interest to explore the potential mechanisms by which methacrolein-derived epoxide
28 intermediates, such as MAE, may lead to the previously observed methacrolein backbone-
29 containing SOA components (i.e., 2-MG-related species).

30

31 In this paper, we report measurements of the bulk-phase reaction of MAE with a number of
32 atmospherically relevant nucleophiles (including MAE itself and 2-MG), using nuclear

1 magnetic resonance (NMR) as the analytic technique. The mechanistic and kinetic data
2 obtained from these experiments are then used to assess the potential nature of MAE reaction
3 on ambient SOA.

4

5 **2 Experimental**

6 **2.1 Synthesis of reactants**

7 **2.1.1 Synthesis of MAE**

8 Both MAE and 2-MG were synthesized following a procedure previously developed to
9 synthesize 2-MG (Birdsall et al., 2013). All precursor compounds were obtained from Sigma-
10 Aldrich and used as obtained, with given purities, unless otherwise noted. Methacrylic acid
11 (MA) (99%, 20 mL, 1 equiv) was added to a 500 mL round-bottom flask containing reagent-
12 grade dichloromethane (200 mL) and a magnetic stir bar. An excess of *meta*-
13 chloroperoxybenzoic acid (*m*CPBA) ($\leq 77\%$, 55 g, 1.25 equiv) was then added as the oxidant.
14 Monitoring the reaction progress with ^1H NMR showed complete epoxidation was achieved
15 after 7 days of stirring at room temperature (22 °C), or 24 h under reflux (40 °C). After
16 filtering off excess *m*CPBA (and the oxidation product *meta*-chlorobenzoic acid (*m*CBA))
17 with successive vacuum filtration and gravity filtration steps until the solution contained no
18 visible precipitate, the crude, dilute epoxide product was divided into two fractions of equal
19 volume: one fraction was worked up to provide purified MAE, while in the other fraction, the
20 MAE was hydrolyzed and isolated to provide 2-MG.

21

22 In order to isolate MAE, further extraction and purification steps were performed, following a
23 literature procedure (Grill et al., 2006). Complete rotary evaporation of dichloromethane
24 resulted in a white slurry. The slurry was transferred to a flask with a minimum of cold (0 °C)
25 deionized water (approximately 40 mL) and briefly swirled by hand. Because MAE is quite
26 water soluble, it partitioned into the aqueous phase. The remaining solid (presumably *m*CBA)
27 was removed via consecutive vacuum and gravity filtration steps and discarded. The
28 remaining aqueous solution underwent rotary evaporation (15 torr pressure, 40 °C bath) until
29 no further volume loss was observed, resulting in a clear, viscous liquid.

30

1 In part because the ^1H NMR spectrum revealed that the aqueous extraction resulted in
2 significant hydrolysis of MAE to 2-MG, MAE was then isolated using flash column
3 chromatography (Costa et al., 2013) with diethyl ether (Fisher Scientific) as the eluent. The
4 isolated MAE was confirmed to be >95% pure by ^1H NMR. Due to the observed slow self-
5 reaction of MAE at room temperature, MAE was stored at $-80\text{ }^\circ\text{C}$ when not in use.

6 **2.1.2 Synthesis of 2-MG**

7 2-MG was formed from the other fraction of dilute, crude MAE by simultaneous aqueous
8 extraction and acid-catalyzed hydrolysis, as described previously (Birdsall et al., 2013). In
9 some cases, a solid was observed to have precipitated out of the crude MAE solution during
10 storage. In this case, another gravity filtration was performed before proceeding with the
11 hydrolysis procedure. The solution was then transferred to an Erlenmeyer flask, and 50 mL of
12 0.2 M HClO_4 (prepared from 70% HClO_4) was added to the mixture to form a biphasic
13 solution with precipitate formation observed in the interfacial region. The solution was stirred
14 continuously, and if necessary, sparing amounts of additional dichloromethane was added
15 over time as dichloromethane evaporated in order to maintain two clearly defined phases.
16 Over 8 days, MAE partitioned into the aqueous phase and hydrolyzed into 2-MG. The
17 solution was gravity filtered, and the aqueous phase was isolated using a separatory funnel.
18 The strong acid (i.e., HClO_4 but not 2-MG) component of the solution was stoichiometrically
19 neutralized with NaOH solution (97%, 10 mL, 1.0 M). The dilute 2-MG solution was
20 transferred to a glass trap with a magnetic stir bar and attached to a vacuum system. Water
21 was removed by gradually lowering the pressure to <1 torr, with vigorous stirring and
22 immersion in a water bath maintained at 295 K, until no more volume loss or drop in vacuum
23 pressure were observed (at approximately 500-600 millitorr). This endpoint was achieved
24 after approximately 2 h of vacuum pumping. No further purification of the resulting 2-MG
25 was found to be necessary (as in the case of MAE, the purity was in excess of 95%), though
26 as discussed in Birdsall et al., (2013), the self-catalyzed conversion of 2-MG via Fischer
27 esterification to oligomer products was observed to appear with an initial concentration of 2%
28 and roughly 7% after 6 months of storage at room temperature (295 K). To avoid even this
29 very slow process, 2-MG was also stored at $-80\text{ }^\circ\text{C}$ when not in use.

1 2.2 NMR technique

2 A variety of nuclear magnetic resonance (NMR) spectra were collected to identify and
3 quantify the products of reactions of MAE. A 400 MHz Varian NMR spectrometer was used
4 to collect all spectra, using default experimental parameters except where noted. Built-in auto-
5 lock and gradient shim routines were used before collecting each spectrum, except when
6 increased temporal resolution was necessary for kinetics measurements. In these cases, the
7 auto-lock and gradient shim routines were performed only once, immediately before the first
8 of a series of spectra were collected. Chemical shifts were calibrated relative to the solvent
9 HDO peak (4.79 ppm) for all ^1H spectra, and relative to DSS (0.0 ppm) (or by using
10 secondary standards that were referenced to DSS) for all ^{13}C spectra. For experiments
11 performed in aqueous solution, D_2O (Cambridge Isotope Laboratories) was used as a solvent.
12 Deuterated methanol, CD_3OD , and deuterated acetic acid CD_3COOD (both Cambridge
13 Isotope Laboratories) were also used as solvents (and nucleophiles) in some experiments, as
14 well.

15
16 The kinetics of MAE hydrolysis were determined using an NMR-based technique previously
17 developed in our lab (Darer et al., 2011; Birdsall et al., 2013). For these experiments, ^1H
18 spectra were collected with 8 scans (30 s) which gave large enough signal-to-noise ratios to
19 be able to follow MAE reactant loss over more than an order of magnitude of relative
20 concentration.

21
22 Product studies of reactions of MAE required the collection of 1D ^{13}C NMR spectra, as well
23 as several 2D spectroscopic techniques: ^1H - ^1H correlation spectroscopy (COSY), ^1H - ^{13}C
24 Heteronuclear Multiple Quantum Correlation spectroscopy (HMQC), and ^1H - ^{13}C
25 Heteronuclear Multiple Bond Coherence spectroscopy (HMBC) (Braun et al., 1998). This
26 suite of NMR experiments provided information about single- and multiple-bond couplings
27 necessary to determine bond connectivity in product molecules and resolve overlapping peaks
28 in 1D NMR spectra.

29
30 Built-in pulse sequences were used for all experiments; an increased number of scans were
31 often used to enhance the signal-to-noise. COSY spectra were collected using the gDQCOSY

1 pulse sequence, which includes both a double-quantum filter and a gradient pulse for
2 improved signal and fewer artifacts. The pulse sequences used to collect HMQC and HMBC
3 spectra, gHMQC and gHMBCAD, respectively, both contained a gradient pulse as well, while
4 the gHMBCAD sequence also included an adiabatic pulse. When necessary to enhance the
5 resolution and signal of HMBC and HMQC spectra, the number of increments and
6 scans/increment were increased from the defaults, up to a maximum of 1024 increments and
7 32 scans/increment. For experiments querying carbon atoms (1D ^{13}C NMR, HMBC), the
8 spin-lattice relaxation time (T1) was increased when necessary, from 1 s to 2-10 s, to improve
9 the signal strength of quaternary carbon peaks.

10 **2.3 MAE hydrolysis kinetics**

11 The kinetics of MAE hydrolysis was measured by using ^1H NMR to monitor the hydrolysis of
12 MAE to 2-MG of solutions containing known amounts of MAE, water, and acid. For each
13 hydrolysis kinetics experiment, 10 μL of MAE was dissolved in 990 μL of 0.10-1.0 M D_2SO_4
14 in D_2O in a 10 mL beaker, with stirring, for 2-3 min. The 1 mL solution was then transferred
15 to a 5 mm NMR tube and ^1H spectra were collected as the hydrolysis progressed, with the
16 time intervals between spectral collection adjusted according to the rate of the reaction.

17 **2.4 MAE nucleophilic addition product identification and relative nucleophilicity** 18 **determination methods**

19 **2.4.1 Deuterated solvent nucleophiles/direct NMR analysis method**

20 For the cases where deuterated nucleophiles were available, MAE was added to the deuterated
21 nucleophile solutions and the reaction was directly monitored in the NMR tube in a process
22 very similar to the method used for the hydrolysis kinetics study.

23

24 Three experimental solutions were prepared (the compositions of the various solutions are
25 given in Table 1): To assess the relative nucleophilicity of sulfate and water in their reactions
26 with MAE, a solution consisting of 10 μL of MAE and 600 μL of 1 M D_2SO_4 in D_2O was
27 prepared (experiment #1). To assess the relative nucleophilicity of acetic acid and water in
28 their reactions with MAE, a solution consisting of 10 μL of MAE and 1000 μL of an
29 equimolar $\text{CD}_3\text{COOD}/\text{D}_2\text{O}$ solution was prepared (experiment #2). To assess the relative

1 nucleophilicity of acetic acid and methanol in their reactions with MAE, a solution consisting
2 of 50 μL of MAE and 1000 μL of an equimolar $\text{CD}_3\text{COOD}/\text{CD}_3\text{OD}$ solution was prepared
3 (experiment #3). Upon the addition of MAE, the solutions were stirred for 2-3 min, at which
4 point the samples were transferred to 5 mm NMR tubes and spectra were collected.

5 **2.4.2 Normal isotope nucleophiles/aliquot NMR analysis method**

6 For the cases where deuterated nucleophiles were not available, MAE was added to the
7 normal isotope nucleophile solution, stirred for 2-3 minutes, and the reaction mixture was
8 stored in a vial at room temperature. Small volume aliquots of these solutions were
9 periodically withdrawn from the vials, added to about 700 μL of D_2O , and the resulting
10 mixtures were loaded into NMR tubes and spectra were collected.

11
12 Four experimental solutions (Table 1) were prepared: To assess the potential oligomer
13 forming reactions of MAE, a neat MAE sample was monitored (experiment #4). To assess
14 the relative nucleophilicity of MAE and 2-MG in their reactions with MAE, a solution
15 consisting of 50 μL of MAE and 0.551 g of 2-MG was prepared (experiment #5). To assess
16 the relative nucleophilicity of MAE and water in their reactions with MAE, a solution
17 consisting of 300 μL of MAE and 29 μL of water (a 2:1 MAE/ H_2O molar ratio) was prepared
18 (experiment #6). To assess the relative nucleophilicity of 2-MG and methanol in their
19 reactions with MAE, a solution consisting of 40 μL of MAE and 0.788 g of an equimolar 2-
20 MG/ H_2O solution that had a small amount of methanol added (the actual methanol content of
21 the solution was determined via NMR methods) was prepared (experiment #7).

22

23 **3 Results**

24 **3.1 MAE and 2-MG NMR identification**

25 ^1H NMR peak assignments for the species observed in the MAE hydrolysis experiments were
26 consistent with the MAE assignments (Lin et al., 2013) and 2-MG assignments (Birdsall et
27 al., 2013) previously reported. As discussed in the Supplement to Birdsall et al., 2013, sets of
28 peaks postulated to arise from diastereomers were observed in the ^1H and ^{13}C spectra in a
29 manner that is consistent with the observations of Espartero et al. (1996) for similar lactic
30 acid-derived species. The complete ^1H and ^{13}C chemical shift assignments for MAE and 2-
31 MG are given in Figures 1 and 2, respectively.

1 3.2 MAE hydrolysis kinetics

2 The rate-determining step of acid-catalyzed epoxide hydrolysis is typically the opening of the
3 epoxide ring, preceded by protonation of the epoxide that acts as a pre-equilibrium step.
4 Because of this pre-equilibrium, the differential rate law can be written in terms of its
5 dependence on H⁺ and MAE

$$-\frac{d[MAE]}{dt} = k[H^+][MAE] \quad (1)$$

6
7 where k is the rate constant, and $[MAE]$ and $[H^+]$ are the molar concentrations of MAE and
8 H⁺, respectively. If the actual acid does not also act as a nucleophile, its concentration is
9 constant over time, allowing for the substitution

$$k' = k[H^+] \quad (2)$$

10
11 where k' is the pseudo-first order rate constant. Sulfuric acid was used the acid source in
12 these experiments. Although deprotonated forms of sulfuric acid can potentially compete
13 with water in the nucleophilic addition process (and thus potentially decrease the acid
14 concentration over time), the use of relatively low concentrations of sulfuric acid led to a
15 situation in which the nucleophilic addition of water dominated for all conditions (as
16 confirmed by the quantification of the nucleophilic addition products formed). Thus, from
17 Eq. 1 and 2 the integrated pseudo-first order rate law is obtained,

$$\ln \frac{[MAE]}{[MAE]_0} = -k't \quad (3)$$

18
19 where $[MAE]_0$ is the initial concentration of MAE. Fig. 3 provides a sample plot of $\ln \frac{[MAE]}{[MAE]_0}$
20 as a function of time, using the relative integrated areas of the methylene protons of 2-MG
21 and MAE in ¹H NMR spectra to calculate $[MAE]/[MAE]_0$.

22
23 The bimolecular rate constant is determined from the extracted k' values over a range of acid
24 concentrations, using the relationship in Eq. 2 (Fig. 4). The range of acidities accessible to our
25 experiments was bounded on the lower end by the increasing significance of the presence of
26 trace sources of acidity (postulated to arise from MAE/2-MG), and on the upper end by the
27 susceptibility of sulfate ester formation at high sulfuric acid concentrations. The extracted rate

1 constant k (and one standard deviation statistical error) was found to be $5.91 \pm 0.45 \times 10^{-5} \text{ M}^{-1}$
2 s^{-1} . Due to possible kinetic isotope effects, the presently reported rate constant (measured in
3 deuterated solvent conditions) may differ from the rate constant appropriate for aerosol
4 environments (normal isotope solvent conditions). While this effect was not investigated in
5 the present study, a previous acid-catalyzed epoxide kinetics investigation (Eddingsaas et al.,
6 2010) estimated that deuterated solvent conditions lead to rate constants that are either equal
7 to those for normal isotope solvent conditions (for SN_2 -like mechanisms) to rate constants as
8 much as a factor of two larger than for normal isotope solvent conditions (for SN_1 -like
9 mechanisms).

10
11 The newly obtained rate constant for MAE hydrolysis can be compared to previously
12 published structure-reactivity trends in bulk phase epoxide hydrolysis kinetics for molecules
13 with alcohol groups (Cole-Filipiak et al., 2010; Minerath et al., 2009). In general, it was found
14 that hydroxyl substitution on a carbon atom adjacent to the epoxide ring reduced the
15 hydrolysis rate constant by up to three orders of magnitude, presumably due to inductive
16 effects that destabilize the carbocation intermediate.

17
18 Table 2 compares the rate constant for MAE hydrolysis to those of other structurally similar
19 epoxides and/or atmospherically relevant epoxides. The epoxide without hydroxyl or carboxyl
20 substitution, 2-methyl-1,2-epoxypropane, has the largest rate constant of all species. The
21 hydroxyl-substituted species, 3-methyl-3,4-epoxy-1,2-butanediol (IEPOX-1) and 2-methyl-
22 2,3-epoxy-1,4-butanediol (IEPOX-4) have rate constants 2-3 orders of magnitude smaller, in
23 line with the predicted structure-reactivity relationship. On the other hand, the carboxyl-
24 substituted species, MAE, has a rate constant more than 600 times smaller than the
25 atmospherically relevant IEPOX-4 species. A recent computational study has predicted that
26 MAE hydrolysis will proceed at a rate 1700 times slower than IEPOX-4 (Piletic et al., 2013),
27 a result in good agreement with the present experimental finding. The computational study
28 also suggested that the reason for the large difference in reactivity is due to a fundamental
29 difference in reaction mechanism: while IEPOX-4 primarily undergoes nucleophilic attack at
30 its tertiary epoxide carbon atom, the computational work suggested that MAE will primarily
31 undergo nucleophilic reaction at its primary epoxide carbon atom.

3.3 Identification of nucleophilic addition mechanisms for MAE reacting with sulfate, methanol, and acetic acid

Figure 5 depicts the two possible generic nucleophilic addition pathways for MAE, one leading to a tertiary addition product, which was not observed in any case, and one leading to a primary addition product, which was observed in every case. For clarity concerning the position of nucleophilic addition, these mechanisms are drawn as sequential reaction (SN_1 -like) mechanisms. While it is likely that these mechanisms are more accurately represented by concerted (SN_2 -like) formalism, the actual mechanism may lie somewhere on a continuum between the sequential and concerted pathways (Whalen, 2005; Eddingsaas et al., 2010; Piletic et al., 2013). It should be noted, however, that the preceding hydrolysis kinetics analysis does not depend on the actual mechanistic pathway (since nucleophilic water is in excess and has an unchanging concentration in those experiments, the two mechanisms are experimentally indistinguishable). Since 2-MG has both alcohol and carboxylic acid functional groups that could potentially act as nucleophiles, methanol and acetic acid were chosen as model systems to explore the similarities and differences for these two different types of nucleophiles. In addition, MAE + sulfate was studied, as 2-MG-related sulfate esters have been identified in previous atmospheric chamber experiments (Gómez-González et al., 2008; Surratt et al., 2007; Hatch et al., 2011a). The NMR evidence for the exclusive presence of a primary addition product for all three nucleophiles - methanol, acetic acid, and sulfate - is discussed in detail below.

3.3.1 MAE + sulfate reaction

This reaction was carried out in a 1 M D_2SO_4 solution (experiment #1), with sulfuric acid serving as both the source of the nucleophilic sulfate ions ($[\text{SO}_4^{2-}] = 0.75$ M according to the Extended Aerosol Inorganics Model (E-AIM) (Clegg et al., 1998)) and the source of acidity ($[\text{D}^+] = 1.2$ M according to E-AIM) needed for catalysis. The relatively fast observed product-forming kinetics indicated that the sulfate ester product was forming as the result of fast MAE + SO_4^{2-} reaction as opposed to slow Fischer esterification 2-MG + SO_4^{2-} reaction (Birdsall et al., 2013). To determine which epoxide carbon the sulfate group had attacked (the two nucleophilic addition pathways shown in Figure 5), the ^1H chemical shifts of the sulfate species was compared to those of 2-MG. The relative CH_3 and CH_2 shifts of the sulfate ester compared to those of 2-MG (~ 0.4 ppm downfield) are the same as the Fischer esterification-

1 produced sulfate ester observed by Birdsall et al., 2013, which was determined through
2 analysis of ^{13}C NMR spectra to be the primary sulfate. Furthermore, based on previous work
3 with sulfates structurally related to 1,2,3,4-butanetetrol, the ^1H NMR spectrum of the tertiary
4 sulfate would be expected to differ significantly, with the CH_2 peaks in the MAE-derived
5 tertiary sulfate expected to appear 0.1 to 0.2 ppm downfield of the 2-MG CH_2 peaks
6 (Minerath and Elrod, 2009). Such peaks were not observed, and thus the NMR evidence
7 points to the exclusive formation ($< 0.5\%$ of initial MAE reactant amount) of a primary
8 sulfate addition product. As discussed in Section 3.2, a previous computational study has
9 identified the primary addition mechanism as the more kinetically facile pathway (Piletic et
10 al., 2013), a finding quite consistent with the present experimental results. The complete ^1H
11 and ^{13}C chemical shift assignments for this species are given in Figures 1 and 2, respectively.

12 **3.3.2 MAE + methanol reaction**

13 In the methanol nucleophile experiments, either CD_3COOD (experiment #3) or 2-MG
14 (experiment #7) provided the acidity needed for the catalysis of the reaction. For the
15 experiment using CD_3OD (experiment #3), new peaks (at 3.45 and 3.75 ppm) located near the
16 2-MG peaks (at 3.60 and 3.82 ppm) were observed, consistent with the formation of a single
17 ether isomer from the nucleophilic addition of methanol to MAE. However, in order to
18 establish the nucleophilic attack position of the methanol moiety, it was also useful to
19 investigate the spectra of the normal isotope (experiment #7). In particular, having
20 observable protons in the ^1H NMR spectrum from the nucleophilic methanol species allowed
21 for long-range coupling between the added methanol moiety and the carbon atom that it
22 attacked in the MAE moiety to be observed. This long-range coupling, observable in an
23 HMBC spectrum, allowed for the definitive structural assignment of a primary or tertiary
24 nucleophilic attack product to be made. In particular, the HMBC spectrum showed a single 3-
25 bond coupling between the protons on the methanol moiety and primary carbon atom on the
26 MAE moiety. Had the tertiary addition product formed, a 3-bond coupling between the
27 protons on the methanol moiety and the tertiary carbon would have been observed in the
28 HMBC spectrum. Therefore, as for the sulfate addition case, the NMR spectrum indicates the
29 sole formation of a methanol primary addition product. The complete ^1H and ^{13}C chemical
30 shift assignments for this species are given in Figures 1 and 2, respectively.

1 **3.3.3 MAE + acetic acid system**

2 In the acetic acid nucleophile experiments, CD₃COOD provided the acidity needed for the
3 catalysis of the reaction. Once again, the NMR evidence showed that the single primary
4 addition species was the sole product formed. The partial ¹H and ¹³C chemical shift
5 assignments for this species are given in Figures 1 and 2, respectively (the acetic acid moiety
6 proton and carbon atoms were not observed due to the exclusive use of CD₃COOD). In the
7 MAE + CD₃COOD/D₂O experiment (experiment #2), the actual pH of the solution could be
8 calculated from the initial concentrations and the known pK_a of acetic acid (pH = 1.8). If the
9 reaction were following a sequential S_{N1}-like mechanism (in which the nucleophile
10 concentration does not affect the overall rate of the reaction), the formal second order rate
11 constant would be expected to be identical to the value determined in the hydrolysis
12 experiment. On the other hand, if the reaction were following a concerted S_{N2}-like
13 mechanism, the phenomenological second order rate constant would be expected to larger
14 if acetic acid were a stronger nucleophile than water, and smaller if acetic acid were a weaker
15 nucleophile than water. The actual second order rate constant determined from experiment #2
16 was 5.0 x 10⁻⁵ M⁻¹ s⁻¹. Since this value is within the experimental uncertainty of the
17 hydrolysis rate constant, an S_{N1}-type mechanism cannot be ruled out. On the other hand,
18 assuming an S_{N2}-type mechanism, this slightly smaller rate constant could be interpreted as
19 indicating that acetic acid is a somewhat weaker nucleophile than water. However, since the
20 reaction may actually be operating along a continuum between the S_{N1}- and S_{N2}-like
21 mechanisms, it is quite difficult to draw any definitive conclusions from this result.

22 **3.4 Identification of nucleophilic addition mechanisms for MAE reacting with** 23 **MAE and 2-MG**

24 Based on the demonstrated preference for MAE to react at its primary epoxide carbon (as
25 outlined above in Section 3.3), it was assumed, as a preliminary analysis provision, that the
26 nucleophiles MAE and 2-MG will also attack exclusively at the MAE primary carbon. Figure
27 6 depicts the specific nucleophilic addition of one MAE molecule acting as a nucleophile
28 (through the OH group on its carboxylic acid moiety) to another MAE molecule. This
29 particular mechanism is capable of producing the kind of higher order oligomers (via chain
30 reaction of the epoxy ester products with MAE) observed in previous environmental chamber
31 studies (Zhang et al., 2011; Chan et al., 2010a; Nguyen et al., 2011). Figure 7 depicts the
32 three possible specific nucleophilic addition options for a 2-MG molecule attacking MAE. If

1 2-MG uses its carboxylic acid OH group, a primary diester (a molecule in which two 2-MG
2 subunits are connected via a single ester linkage) would be expected to form (this particular
3 species can also be produced via the acid-catalyzed Fischer self-esterification of 2-MG, a
4 process previously studied in our lab (Birdsall et al., 2013)). On the other hand, if 2-MG uses
5 either of its alcoholic OH groups, either a primary or a tertiary diether (molecules in which
6 two 2-MG subunits are connected via a single ether linkage) would be expected to form. The
7 nomenclature used to identify the various species in Figures 1,2,6 and 7 is intended to
8 highlight the mechanistic route by which the species formed. For example, the *primary*
9 *diester* name assigned to the species formed as shown at the bottom of Figure 7 reflects that
10 this *dimeric* species (formed from the reaction of MAE with 2-MG) is connected via a single
11 *ester* linkage that formed at the *primary* epoxide carbon of MAE.

12
13 For the MAE + MAE reaction (experiment #4), MAE provided the acidity needed for the
14 catalysis of the reaction, while in the MAE + 2-MG reactions (experiments #5 and #7), 2-MG
15 provided the acidity. Due to the presence of unavoidable water impurity in the MAE sample,
16 the "neat" MAE reaction system (experiment #4) is actually the most complicated one, since
17 MAE can react with itself, water, 2-MG (formed from reaction of MAE with water), which
18 were all present in significant concentrations in experiment #4 (indeed, some of the products
19 of these reactions were identified as participating in further reactions further adding to the
20 number of observed species). However, with the aid of experiments in which the relative
21 MAE:water:2-MG amounts were changed (experiments #5 and #6), all of the various
22 products were identified and quantified. The carbonyl region of the ¹³C NMR spectrum for
23 experiment #4 is shown in Figure 8 for the two conditions of early reaction (most MAE is still
24 unreacted) and late reaction (most MAE has reacted). During the early phase of the reaction,
25 both the epoxy diester and 2-MG are observed products: 2-MG is formed via hydrolysis from
26 the water impurity in the neat MAE sample, while the epoxy diester is formed from the MAE
27 + MAE mechanism shown in Figure 5. During the late reaction phase, the epoxy triester is
28 observable (formed from the reaction of the epoxy diester + MAE, as shown in Figure 6), in
29 addition to two of the species shown in Figure 7: the primary diether species (formed from
30 MAE reaction with the primary OH group acting as a nucleophilic group on 2-MG) and the
31 primary diester species. The triester (formed from the reaction of the epoxy diester with 2-
32 MG) is also evident in the late reaction phase spectrum. The tertiary diether species was not

1 observed (were it present in the NMR spectrum, it could be easily distinguished from the
2 primary diether because of its asymmetric structure).

3

4 Since the diester species could be formed from either 1) MAE reaction with the carboxylic
5 acid OH of 2-MG (as shown in Figure 7) or from 2) hydrolysis of the epoxy diester (as
6 shown in Figure 9), further experiments were necessary to identify the relevant mechanisms.
7 In order to isolate the MAE + 2-MG (carboxylic acid nucleophile) diester-forming pathway
8 and to measure the relative nucleophilicity of 2-MG using its carboxylic acid moiety vs.
9 alcohol moiety, an experiment was performed in which 2-MG was placed in excess over the
10 water impurity (experiment #5). Based on NMR quantitation, it was found that the MAE + 2-
11 MG (carboxylic acid nucleophile) and MAE + 2-MG (alcohol nucleophile) reaction pathways
12 are equally facile (of the total 0.19 mole fraction MAE + 2-MG products, 0.10 mole fraction
13 was attributable to the diester product and 0.09 mole fraction was attributable to the diether
14 product). In experiment #6, additional water was intentionally added to favor the formation
15 of the diester via the hydrolysis of the epoxy diester species. NMR quantitation for this
16 experiment indicated that while 0.03 mole fraction of the diether formed (via the MAE + 2-
17 MG (alcohol nucleophile) pathway), 0.24 mole fraction of the diester formed. Since
18 experiment #5 indicated that the MAE + 2-MG (carboxylic acid nucleophile) pathway is
19 expected to produce the diester in the same amounts as the diether, it can be assumed that the
20 extra 0.21 mole fraction of diester formed in experiment #6 is due to the hydrolysis of the
21 epoxy diester. Therefore, it is quite likely that the diester product observed in experiment #4
22 (and identified in Figure 8) is produced from both the MAE + 2-MG (carboxylic acid
23 nucleophile) and the epoxy diester + H₂O reactions.

24

25 While the NMR spectra of the diester were previously reported in the context of the acid-
26 catalyzed Fischer esterification of 2-MG (Birdsall et al., 2013), the newly observed epoxy
27 diester and the primary diether species were definitively assigned by using experimental
28 conditions which favored their formation (experiments #4 and #5, respectively), and with the
29 aid of HMQC and HMBC correlation experiments. (These experiments also confirmed that all
30 species were the result of nucleophilic attack on the MAE primary carbon, as expected.) The
31 complete ¹H and ¹³C chemical shift assignments for these species are given in Figures 1 and

1 2, respectively. Due to spectral overlap complications, complete triester and epoxy triester
2 assignments were not obtained.

3

4 **3.5 Relative nucleophilicity scale**

5 Using the initial nucleophilic reactant mole fractions (X, determined via volume and/or mass
6 measurements) and the final nucleophilic addition product mole fractions (Y, determined via
7 NMR quantitation methods) listed in Table 1, it is possible to determine the relative
8 nucleophilicities (on a molar basis) for the reaction of MAE with the various nucleophiles via
9 Equation 4:

$$\frac{\text{nucleophile 1 strength}}{\text{nucleophile 2 strength}} = \frac{(Y_{nuc\ 1}/X_{nuc\ 1})}{(Y_{nuc\ 2}/X_{nuc\ 2})} \quad (4)$$

10

11 Note that in some of the experiments, more than two nucleophiles were present (which is why
12 the mole fractions in Table 1 don't necessarily sum to unity). It is further possible to relate
13 the nucleophilic strength of all nucleophiles to that of MAE. Starting with experiments #5
14 and #6, the relative nucleophilic strengths of 2-MG and water to MAE are established (1.2
15 and 1.6, respectively). Next, the nucleophilic strengths (relative to MAE) of the other
16 nucleophiles are established via their strengths relative to 2-MG and water. In the case of
17 methanol, there are two experiments which can be used to calculate the relative
18 methanol/MAE nucleophilicity; in this case an average value is calculated. Table 2 gives the
19 relative nucleophilic strengths of all studied nucleophiles in their reactions with MAE. In a
20 previous computational study of MAE reactivity, it was predicted that the MAE relative (to
21 water) nucleophilicities for SO_4^{2-} and propanol were 9.8 and 3.6, respectively (Piletic et al.,
22 2013). Converting the values given in Table 1 to nucleophilicities relative to water for
23 comparison purposes, the experimental nucleophilicities for SO_4^{2-} and methanol were
24 determined to be 11 and 3.1, respectively, which are in good agreement with the
25 computational predictions. Interestingly, while the relative nucleophilicity of 2-MG using its
26 carboxylic acid moiety was experimentally found to be similar to that of acetic acid, the
27 experimental relative nucleophilicity of 2-MG using its alcohol moiety was found to be
28 significantly less than methanol. Therefore, while the experimental results indicate that the
29 nucleophilicity of multifunctional molecules like 2-MG may be approximately viewed as the

1 sum of the nucleophilic strength of separate nucleophilic functional groups, the results also
2 indicate that caution should be used in this simplifying approach.

3

4 **4 Atmospheric implications**

5 **4.1 MAE reaction feasibility on SOA**

6 Using a previously described framework to estimate the kinetics feasibility of acid-catalyzed
7 epoxide reactions on SOA (Cole-Filipiak et al., 2010), the lifetime, τ , of MAE reaction over a
8 range of atmospherically relevant pHs was calculated using the equation

$$\tau = [H^+]^{-1}k^{-1} \quad (5)$$

9

10 Using the newly determined experimental MAE reaction rate constant results, Equation 5
11 yields lifetimes of 2.0×10^3 days at pH = 4.0, 6.2 days at pH = 1.5, and 0.20 days at pH = 0.
12 Thus, over a range of atmospherically relevant pHs (Zhang et al., 2007), the expected lifetime
13 of MAE reaction can range above and below the average lifetime of an aerosol particle (on
14 the order of 2 days). The finding that MAE reaction is kinetically feasible under
15 atmospherically relevant conditions is consistent with the observation of both the hydrolysis
16 product, 2-MG, and—as reported more recently in Lin et al., 2013—the reactant, MAE, on
17 ambient SOA. While the MAE reaction route to oligomers was found to be about 30 times
18 faster than the Fischer esterification route previously investigated (Birdsall et al., 2013), the
19 MAE reaction is much slower than that of the atmospherically relevant IEPOX-4 species (by
20 a factor of 620, Table 2). A previous atmospheric modeling study of the role of IEPOX and
21 MAE assumed, in the absence of experimental data, that the rate constants for the two species
22 were identical (Pye et al., 2013). Clearly, the much smaller rate constant for MAE will need
23 to be included in future modeling efforts, with the result that modeled MAE reactivity will
24 likely be reduced.

25 **4.2 MAE oligomerization mechanism on SOA**

26 In previous work (Lin et al., 2013), it had been shown that MAE reactions on SOA are
27 capable of producing the kind of 2-MG subunit-containing oligomers identified in
28 environmental chamber experiments (Zhang et al., 2011; Chan et al., 2010a; Nguyen et al.,
29 2011). In this work, we have identified the specific mechanism (epoxy ester chain reaction,

1 as given in Fig. 6) by which MAE reactions lead to such oligomers. While there are
2 potentially two reaction sites for this oligomerization reaction on the epoxide reactant (the
3 primary or tertiary carbon), this work has shown that MAE appears to exclusively react via its
4 primary carbon atom with all studied nucleophiles (including the MAE unit acting as the
5 nucleophile in the oligomerization chain reaction). Therefore, this result leads to the
6 prediction that each higher order oligomer will consist of a single isomer, possessing an
7 extended open chain structure, owing to the exclusive primary reaction site mechanism.

8 **4.3 MAE nucleophilic reactions on SOA**

9 The products and nucleophilic strengths of a number of MAE + nucleophile reactions were
10 determined in order to assess the likelihood of MAE reaction with a number of
11 atmospherically-relevant nucleophilic classes of species: HOH, ROH, RC(=O)OH and sulfate.
12 The product studies confirmed that MAE can react with each of the classes to form diol, ether,
13 diester, and sulfate ester species, respectively. This work also showed that 2-MG, a
14 dihydroxy acid, can react using both its primary alcoholic OH (to form an ether product) and
15 carboxylic OH (to form an ester product) groups as nucleophilic agents. The measured
16 relative nucleophilic strengths of the MAE reaction with the various species indicates that
17 MAE itself is not a particularly strong nucleophile. Thus, it is then straightforward to
18 rationalize why extensive oligomerization has been observed only for laboratory experiments
19 under conditions of low SOA water content: at high SOA water content, water successfully
20 competes with MAE as a nucleophile, and limits oligomerization by direct hydrolysis of MAE
21 or by hydrolysis of the epoxy diester species (as shown in Fig. 9) that is one of the chain
22 carriers in the oligomerization chain reaction. In ambient SOA, other effective nucleophiles
23 may be present in high concentrations (such as alcohols, acids, and inorganic ions), and MAE
24 reactions with these species could also be competitive with hydrolysis and/or oligomerization
25 mechanistic pathways. Therefore, the nature of MAE reaction on SOA is expected to depend
26 sensitively on the chemical composition of the preexisting SOA particle; for cases with
27 heterogeneous SOA compositions, a variety of MAE-derived products may be expected, with
28 these reactions likely outcompeting the oligomerization pathways (due to MAE's mediocre
29 nucleophilic strength and relatively low concentration compared to such abundant
30 nucleophiles such as water and sulfate). While the nitrate nucleophile was not directly
31 studied in these experiments, because its relative nucleophilicity has been found to be similar
32 to sulfate for reactions with isoprene-derived epoxides (Darer et al., 2011), it is expected that

1 for MAE reactions that sulfate and nitrate would have similarly nucleophilicities. While
2 hetero-oligomers, formed from cross reactions of MAE with other atmospherically relevant
3 epoxides (such as IEPOX and 2-methyl-3-buten-2-ol-derived (Zhang et al., 2014) epoxides),
4 might be formed on ambient SOA, these epoxides are also expected to have mediocre
5 nucleophilic strength (they are probably more similar to 2-MG than to methanol) and these
6 reactions would also probably not be competitive with reactions involving more abundant
7 nucleophiles. Thus far, field studies have identified only two likely MAE reaction products,
8 2-MG and the diester (Jaoui et al., 2008), which are likely formed from hydrolysis of MAE
9 and the reaction of MAE with 2-MG, respectively. The formation of the diester from the
10 epoxy diester hydrolysis reaction on ambient SOA is less likely since conditions favoring
11 hydrolysis would also favor the formation of 2-MG, which would probably lead to the
12 dominance of the MAE + 2-MG diester-forming pathway.

13

14 **5 Conclusions**

15 The present results suggest that acid-catalyzed nucleophilic addition to MAE is much slower
16 than the analogous IEPOX-4 reaction, but, nonetheless, is expected to be kinetically feasible
17 in the atmosphere, particularly on more acidic SOA. The specific mechanism by which
18 MAE leads to oligomers was identified (epoxide chain reaction), and the reactions of MAE
19 with a number of atmospherically relevant nucleophiles were also investigated. Because the
20 nucleophilic strengths of water, sulfate, alcohols (including 2-MG), and acids (including
21 MAE and 2-MG) in their reactions with MAE were found to be of a similar magnitude, it is
22 expected that a diverse variety of MAE + nucleophile product species may be formed on
23 ambient SOA. Thus, the results indicate that epoxide chain reaction oligomerization will be
24 limited by the presence of high concentrations of non-epoxide nucleophiles (such as water);
25 this finding is consistent with previous environmental chamber investigations of the relative
26 humidity-dependence of 2-MG-derived oligomerization processes and suggests that extensive
27 oligomerization may not be likely on ambient SOA because of other competitive MAE
28 reaction mechanisms..

29

30 **Acknowledgements**

31 This work was supported by the National Science Foundation under Grant No. 1153861.

32

1 References

- 2 Birdsall, A. W., Zentner, C. A., and Elrod, M. J.: Study of the kinetics and equilibria of the
3 oligomerization reactions of 2-methylglyceric acid, *Atmos. Chem. Phys.*, 13, 3097-3109,
4 10.5194/acp-13-3097-2013, 2013.
- 5 Carlton, A. G., Wiedinmyer, C., and Kroll, J. H.: A review of secondary organic aerosol
6 (SOA) formation from isoprene, *Atmos. Chem. Phys.*, 9, 4987-5005, 2009.
- 7 Chan, A. W. H., Chan, M. N., Surratt, J. D., Chhabra, P. S., Loza, C. L., Crouse, J. D., Yee,
8 L. D., Flagan, R. C., Wennberg, P. O., and Seinfeld, J. H.: Role of aldehyde chemistry and
9 NO_x concentrations in secondary organic aerosol formation, *Atmos. Chem. Phys.*, 10, 7169-
10 7188, 10.5194/acp-10-7169-2010, 2010a.
- 11 Chan, M. N., Surratt, J. D., Claeys, M., Edgerton, E. S., Tanner, R. L., Shaw, S. L., Zheng,
12 M., Knipping, E. M., Eddingsaas, N. C., Wennberg, P. O., and Seinfeld, J. H.:
13 Characterization and quantification of isoprene-derived epoxydiols in ambient aerosol in the
14 southeastern United States, *Environ. Sci. Technol.*, 44, 4590-4596, 2010b.
- 15 Clegg, S. L., Brimblecombe, P., and Exler, A. S.: A thermodynamic model of the system H^+ -
16 NH_4^+ - SO_4^{2-} - NO_3^- - H_2O at tropospheric temperatures, *J. Phys. Chem. A*, 102, 2137-2154, 1998.
- 17 Cole-Filipiak, N. C., O'Connor, A. E., and Elrod, M. J.: Kinetics of the hydrolysis of
18 atmospherically relevant isoprene-derived hydroxy epoxides, *Environ. Sci. Technol.*, 44,
19 6718-6723, 2010.
- 20 Costa, V. V., da Silva Rocha, K. A., Kozhevnikov, I. V., Kozhevnikova, E. F., and
21 Gusevskaya, E. V.: Heteropoly acid catalysts for the synthesis of fragrance compounds from
22 biorenewables: isomerization of limonene oxide, *Catalysis Science & Technology*, 3, 244-
23 250, 10.1039/c2cy20526b, 2013.
- 24 Darer, A. I., Cole-Filipiak, N. C., O'Connor, A. E., and Elrod, M. J.: Formation and stability
25 of atmospherically relevant isoprene-derived organosulfates and organonitrates, *Environ. Sci.*
26 *Technol.*, 45, 1895-1902, 2011.
- 27 Eddingsaas, N. C., VanderVelde, D. G., and Wennberg, P. O.: Kinetics and products of the
28 acid-catalyzed ring-opening of atmospherically relevant butyl epoxy alcohols, *J. Phys. Chem.*
29 *A*, 114, 8106-8113, Doi 10.1021/Jp103907c, 2010.
- 30 Edney, E., Kleindienst, T., Jaoui, M., Lewandowski, M., Offenber, J., Wang, W., and
31 Claeys, M.: Formation of 2-methyl tetrols and 2-methylglyceric acid in secondary organic
32 aerosol from laboratory irradiated isoprene/NO/SO/air mixtures and their detection in ambient
33 PM samples collected in the eastern United States, *Atmos. Environ.*, 39, 5281-5289,
34 10.1016/j.atmosenv.2005.05.031, 2005.
- 35 Gómez-González, Y., Surratt, J. D., Cuyckens, F., Szmigielski, R., Vermeylen, R., Jaoui, M.,
36 Lewandowski, M., Offenber, J. H., Kleindienst, T. E., Edney, E. O., Blockhuys, F., Van
37 Alsenoy, C., Maenhaut, W., and Claeys, M.: Characterization of organosulfates from the
38 photooxidation of isoprene and unsaturated fatty acids in ambient aerosol using liquid
39 chromatography/(-) electrospray ionization mass spectrometry, *J. Mass Spectrom.*, 43, 371-
40 382, 10.1002/jms.1329, 2008.
- 41 Grill, J. M., Ogle, J. W., and Miller, S. A.: An Efficient and Practical System for the Catalytic
42 Oxidation of Alcohols, Aldehydes, and α,β -Unsaturated Carboxylic Acids, *The Journal of*
43 *Organic Chemistry*, 71, 9291-9296, 10.1021/jo0612574, 2006.

1 Hallquist, M., Wenger, J. C., Baltensperger, U., Rudich, Y., Simpson, D., Claeys, M.,
2 Dommen, J., Donahue, N. M., George, C., Goldstein, A. H., Hamilton, J. F., Herrmann, H.,
3 Hoffmann, T., Iinuma, Y., Jang, M., Jenkin, M. E., Jimenez, J. L., Kiendler-Scharr, A.,
4 Maenhaut, W., McFiggans, G., Mentel, T. F., Monod, A., Prevot, A. S. H., Seinfeld, J. H.,
5 Surratt, J. D., Szmigielski, R., and Wildt, J.: The formation, properties and impact of
6 secondary organic aerosol: current and emerging issues, *Atmos. Chem. Phys.*, 9, 5155-5236,
7 2009.

8 Hatch, L. E., Creamean, J. M., Ault, A. P., Surratt, J. D., Chan, M. N., Seinfeld, J. H.,
9 Edgerton, E. S., Su, Y., and Prather, K. A.: Measurements of isoprene-derived organosulfates
10 in ambient aerosols by aerosol time-of-flight mass spectrometry - part 1: single particle
11 atmospheric observations in Atlanta, *Environ. Sci. Technol.*, 45, 5105-5111,
12 10.1021/es103944a, 2011a.

13 Hatch, L. E., Creamean, J. M., Ault, A. P., Surratt, J. D., Chan, M. N., Seinfeld, J. H.,
14 Edgerton, E. S., Su, Y., and Prather, K. A.: Measurements of isoprene-derived organosulfates
15 in ambient aerosols by aerosol time-of-flight mass spectrometry—part 2: temporal variability
16 and formation mechanisms, *Environ. Sci. Technol.*, 45, 8648-8655, 10.1021/es2011836,
17 2011b.

18 Hu, K. S., Darer, A. I., and Elrod, M. J.: Thermodynamics and kinetics of the hydrolysis of
19 atmospherically relevant organonitrates and organosulfates, *Atmos. Chem. Phys.*, 11, 8307-
20 8320, 10.5194/acp-11-8307-2011, 2011.

21 Jaoui, M., Edney, E. O., Kleindienst, T. E., Lewandowski, M., Offenber, J. H., Surratt, J. D.,
22 and Seinfeld, J. H.: Formation of secondary organic aerosol from irradiated α -
23 pinene/toluene/NO_x mixtures and the effect of isoprene and sulfur dioxide, *Journal of*
24 *Geophysical Research*, 113, D09303, 10.1029/2007jd009426, 2008.

25 Lin, Y.-H., Zhang, Z., Docherty, K. S., Zhang, H., Budisulistiorini, S. H., Rubitschun, C. L.,
26 Shaw, S. L., Knipping, E. M., Edgerton, E. S., Kleindienst, T. E., Gold, A., and Surratt, J. D.:
27 Isoprene epoxydiols as precursors to secondary organic aerosol formation: acid-catalyzed
28 reactive uptake studies with authentic compounds, *Environ. Sci. Technol.*, 46, 250-258,
29 10.1021/es202554c, 2012.

30 Lin, Y.-H., Zhang, H., Pye, H. O. T., Zhang, Z., Marth, W. J., Park, S., Arashiro, M., Cui, T.,
31 Budisulistiorini, S. H., Sexton, K. G., Vizuete, W., Xie, Y., Luecken, D. J., Piletic, I. R.,
32 Edney, E. O., Bartolotti, L. J., Gold, A., and Surratt, J. D.: Epoxide as a precursor to
33 secondary organic aerosol formation from isoprene photooxidation in the presence of nitrogen
34 oxides, *Proc. Natl. Acad. Sci.*, 110, 6718-6723, 10.1073/pnas.1221150110, 2013.

35 Minerath, E. C., and Elrod, M. J.: Assessing the potential for diol and hydroxy sulfate ester
36 formation from the reaction of epoxides in tropospheric aerosols, *Environ. Sci. Technol.*, 43,
37 1386-1392, 10.1021/es8029076, 2009.

38 Minerath, E. C., Schultz, M. P., and Elrod, M. J.: Kinetics of the reactions of isoprene-derived
39 epoxides in model tropospheric aerosol solutions, *Environ. Sci. Technol.*, 43, 8133-8139,
40 10.1021/es902304p, 2009.

41 Nguyen, T. B., Roach, P. J., Laskin, J., Laskin, A., and Nizkorodov, S. A.: Effect of humidity
42 on the composition and yield of isoprene photooxidation secondary organic aerosol, *Atmos.*
43 *Chem. Phys.*, 11, 6931-6944, 10.5194/acpd-11-9217-2011, 2011.

1 Paulot, F., Crouse, J. D., Kjaergaard, H. G., Kurten, A., St. Clair, J. M., Seinfeld, J. H., and
2 Wennberg, P. O.: Unexpected epoxide formation in the gas-phase photooxidation of isoprene,
3 *Science*, 325, 730-733, 10.1126/science.1172910, 2009.

4 Piletic, I. R., Edney, E. O., and Bartolotti, L. J.: A computational study of acid catalyzed
5 aerosol reactions of atmospherically relevant epoxides, *Phys. Chem. Chem. Phys.*, 15, 18065,
6 10.1039/c3cp52851k, 2013.

7 Pye, H. O. T., Pinder, R. W., Piletic, I. R., Xie, Y., Capps, S. L., Lin, Y.-H., Surratt, J. D.,
8 Zhang, Z., Gold, A., Luecken, D. J., Hutzell, W. T., Jaoui, M., Offenberg, J. H., Kleindienst,
9 T. E., Lewandowski, M., and Edney, E. O.: Epoxide Pathways Improve Model Predictions of
10 Isoprene Markers and Reveal Key Role of Acidity in Aerosol Formation, *Environ. Sci.*
11 *Technol.*, 47, 11056-11064, 10.1021/es402106h, 2013.

12 Surratt, J. D., Murphy, S. M., Kroll, J. H., Ng, N. L., Hildebrandt, L., Sorooshian, A.,
13 Szmigielski, R., Vermeylen, R., Maenhaut, W., Claeys, M., Flagan, R. C., and Seinfeld, J. H.:
14 Chemical Composition of Secondary Organic Aerosol Formed from the Photooxidation of
15 Isoprene, *J. Phys. Chem. A*, 110, 9665-9690, 10.1021/jp061734m, 2006.

16 Surratt, J. D., Kroll, J. H., Kleindienst, T. E., Edney, E. O., Claeys, M., Sorooshian, A., Ng,
17 N. L., Offenberg, J. H., Lewandowski, M., Jaoui, M., Flagan, R. C., and Seinfeld, J. H.:
18 Evidence for organosulfates in secondary organic aerosol, *Environ. Sci. Technol.*, 41, 517-
19 527, 2007.

20 Surratt, J. D., Chan, A. W. H., Eddingsaas, N. C., Chan, M., Loza, C. L., Kwan, A. J., Hersey,
21 S. P., Flagan, R. C., Wennberg, P. O., and Seinfeld, J. H.: Reactive intermediates revealed in
22 secondary organic aerosol formation from isoprene, *Proc. Natl. Acad. Sci.*, 107, 6640-6645,
23 2010.

24 Szmigielski, R., Surratt, J. D., Vermeylen, R., Szmigielska, K., Kroll, J. H., Ng, N. L.,
25 Murphy, S. M., Sorooshian, A., Seinfeld, J. H., and Claeys, M.: Characterization of 2-
26 methylglyceric acid oligomers in secondary organic aerosol formed from the photooxidation
27 of isoprene using trimethylsilylation and gas chromatography/ion trap mass spectrometry, *J.*
28 *Mass Spectrom.*, 42, 101-116, 10.1002/jms.1146, 2007.

29 Whalen, D. L.: Mechanisms of hydrolysis and rearrangements of epoxides, *Adv. Phys. Org.*
30 *Chem.*, 40, 247-298, 2005.

31 Zhang, H., Surratt, J. D., Lin, Y. H., Bapat, J., and Kamens, R. M.: Effect of relative humidity
32 on SOA formation from isoprene/NO photooxidation: enhancement of 2-methylglyceric acid
33 and its corresponding oligoesters under dry conditions, *Atmos. Chem. Phys.*, 11, 6411-6424,
34 10.5194/acp-11-6411-2011, 2011.

35 Zhang, H., Zhang, Z., Cui, T., Lin, Y.-H., Bathela, N. A., Ortega, J., Worton, D. R.,
36 Goldstein, A. H., Guenther, A., Jimenez, J. L., Gold, A., and Surratt, J. D.: Secondary Organic
37 Aerosol Formation via 2-Methyl-3-buten-2-ol Photooxidation: Evidence of Acid-Catalyzed
38 Reactive Uptake of Epoxides, *Environmental Science & Technology Letters*, 1, 242-247,
39 10.1021/ez500055f, 2014.

40 Zhang, Q., Jimenez, J. L., Worsnop, D. R., and Canagaratna, M.: A case study of urban
41 particle acidity and its influence on secondary organic aerosol, *Environ. Sci. Technol.*, 41,
42 3213-3219, 2007.

43
44

1 **Table 1.** Initial reactants mole fractions (X) and final products mole fractions (Y) for the
 2 different experiments performed. The product mole fractions were determined with an
 3 estimated relative error of 25%

4

Exp.	X _{MAE}	Nuc 1	X _{Nuc1}	Nuc 2	X _{Nuc2}	Y _{MAE-MAE}	Y _{MAE-Nuc1}	Y _{MAE-Nuc2}
1	0.003	SO ₄ ²⁻	0.0045	D ₂ O	0.992		0.05	0.95
2	0.005	d-AA ^a	0.492	D ₂ O	0.492		0.28	0.72
3	0.026	d-AA	0.487	d-MeOH ^b	0.487		0.16	0.84
4 ^c	> 0.8							
5	0.110	2-MG	0.890			0.02	0.19	
6	0.670	H ₂ O	0.330			0.33	0.26	
7	0.021	2-MG	0.461	MeOH	0.054		0.09	0.06

5

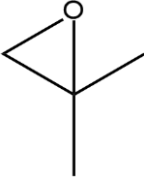
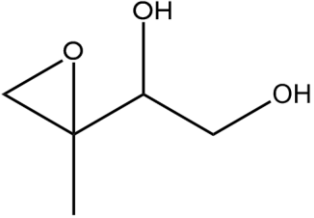
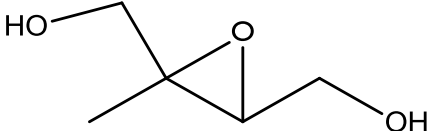
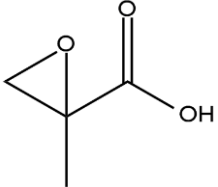
6 ^ad-AA: deuterated acetic acid (CD₃COOD)

7 ^bd-MeOH: deuterated methanol (CD₃OD)

8 ^cExperiment #4 was a “neat” sample of MAE contaminated with at most 0.20 mole fraction
 9 water. Because of the uncertainty in the water content of this sample, Experiment #4 was not
 10 used in the quantitative determination of relative nucleophilities, but rather was used to
 11 establish NMR assignments and to aid in the mechanistic interpretation of the MAE reactions.

1 **Table 2.** Acid-catalyzed rate constants for primary-tertiary epoxide hydrolysis with varying
 2 substitution. ^a(Minerath and Elrod, 2009) ^b(Cole-Filipiak et al., 2010) ^cThis work.

3
 4
 5

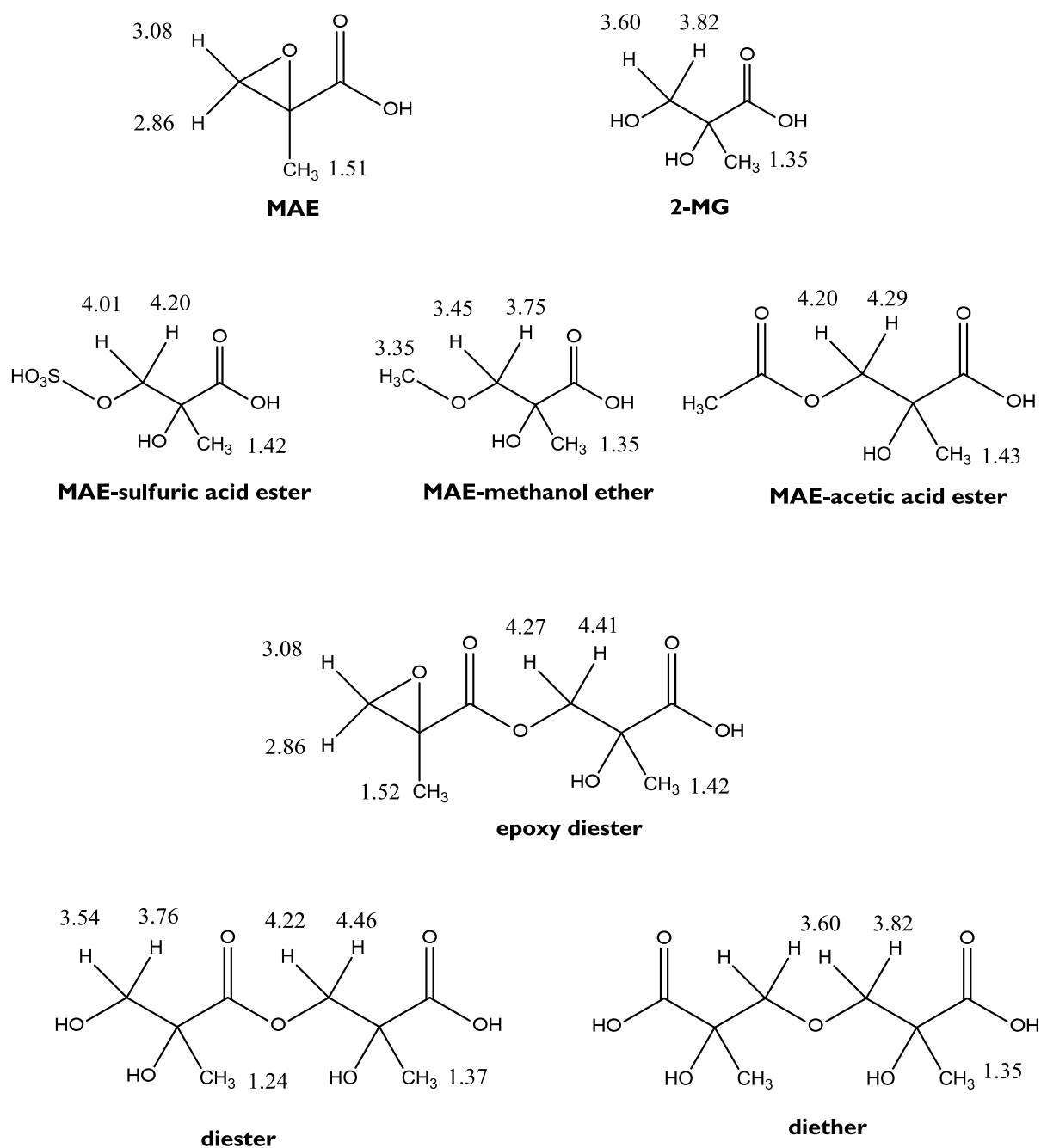
epoxide	k (M ⁻¹ s ⁻¹)
 2-methyl-1,2-epoxypropane	8.7 ^a
 IEPOX-1 (3-methyl-3,4-epoxy-1,2-butanediol)	0.0079 ^b
 IEPOX-4 (2-methyl-2,3-epoxy-1,4-butanediol)	0.036 ^b
 MAE (2-methyl-2,3-epoxypropanoic acid)	0.0000591 ^c

1 **Table 3.** MAE reaction relative nucleophilic strength scale. The relative nucleophilicities
2 were determined with an estimated uncertainty of about 50%, due to uncertainties in both
3 reactant and product mole fraction measurements.

4

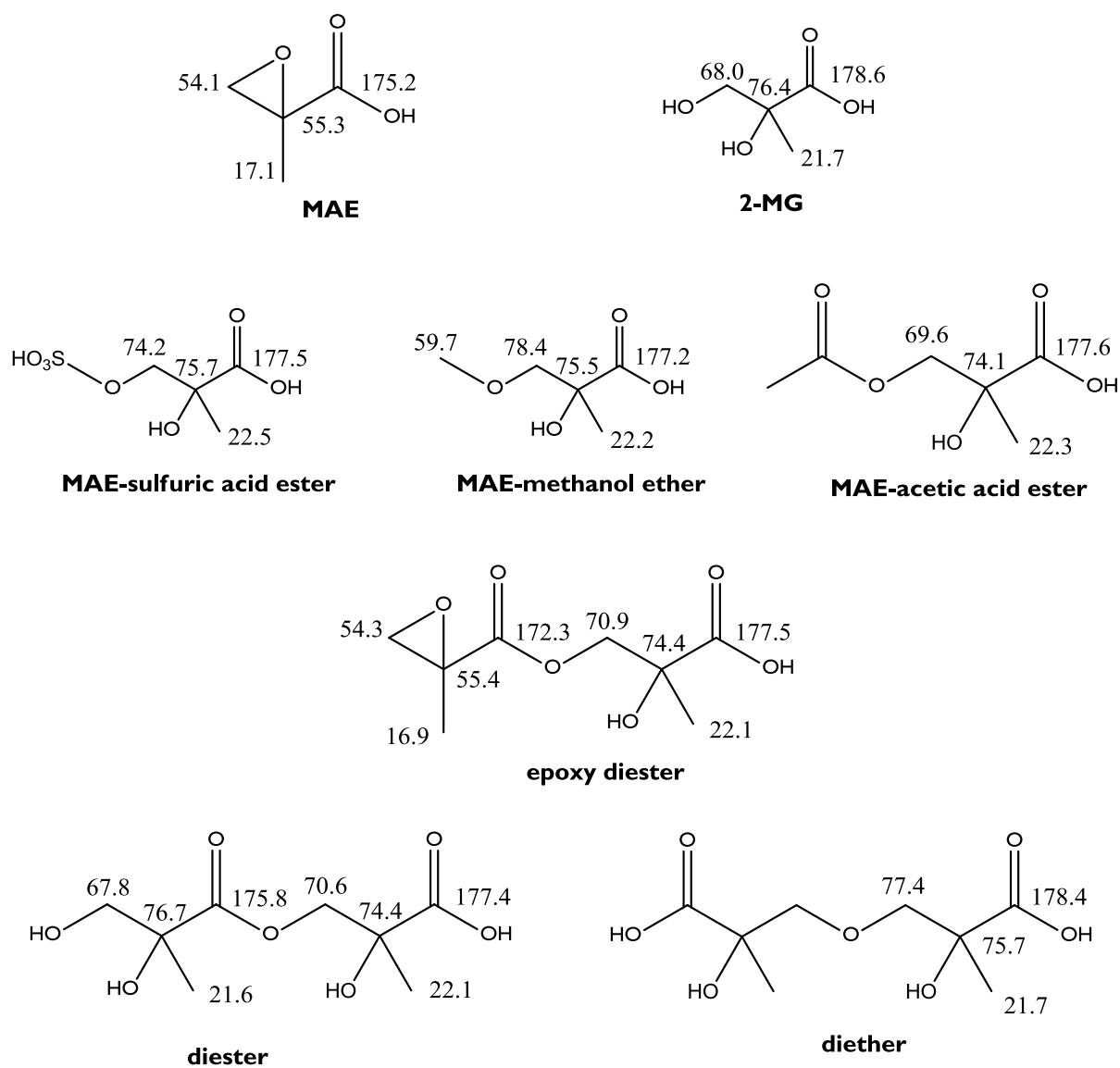
nucleophile	relative nucleophilicity
acetic acid	0.6
MAE	1 (by definition)
2-MG	1.2 total = 0.6 (carboxylic acid) + 0.6 (primary alcohol)
water	1.6
methanol	5.0
SO ₄ ²⁻	18

5



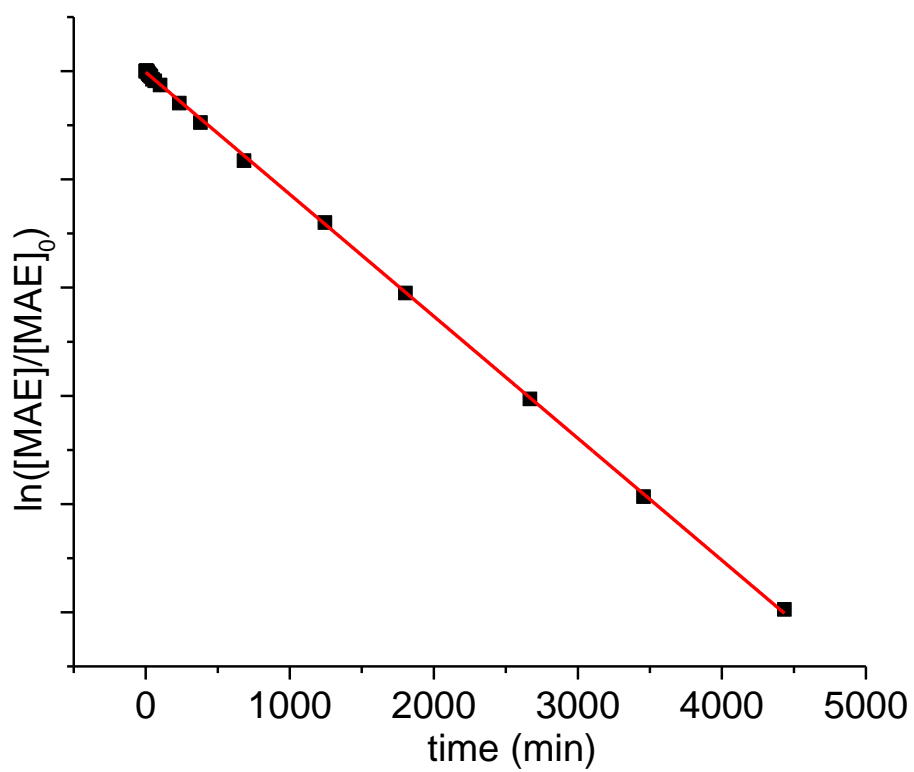
1
2
3

Fig. 1. ¹H NMR chemical shift assignments for MAE-related species.



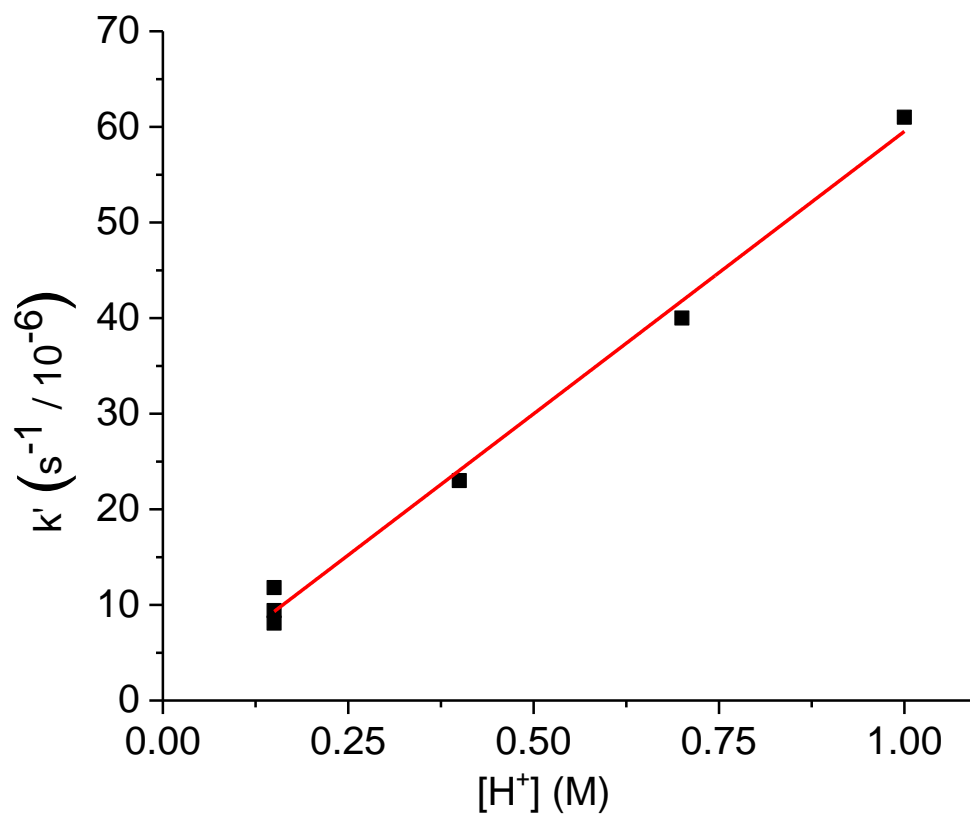
1
2
3

Fig. 2. ^{13}C NMR chemical shift assignments for MAE-related species.



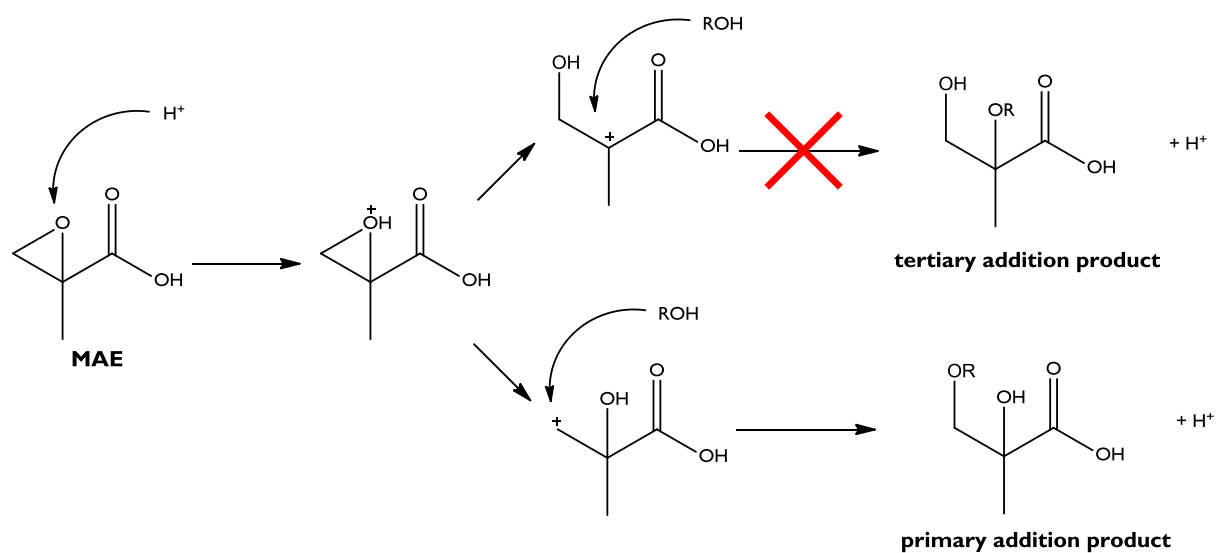
1
2
3

Fig. 3. Pseudo first order decay of MAE in 1.0 M D₂SO₄.



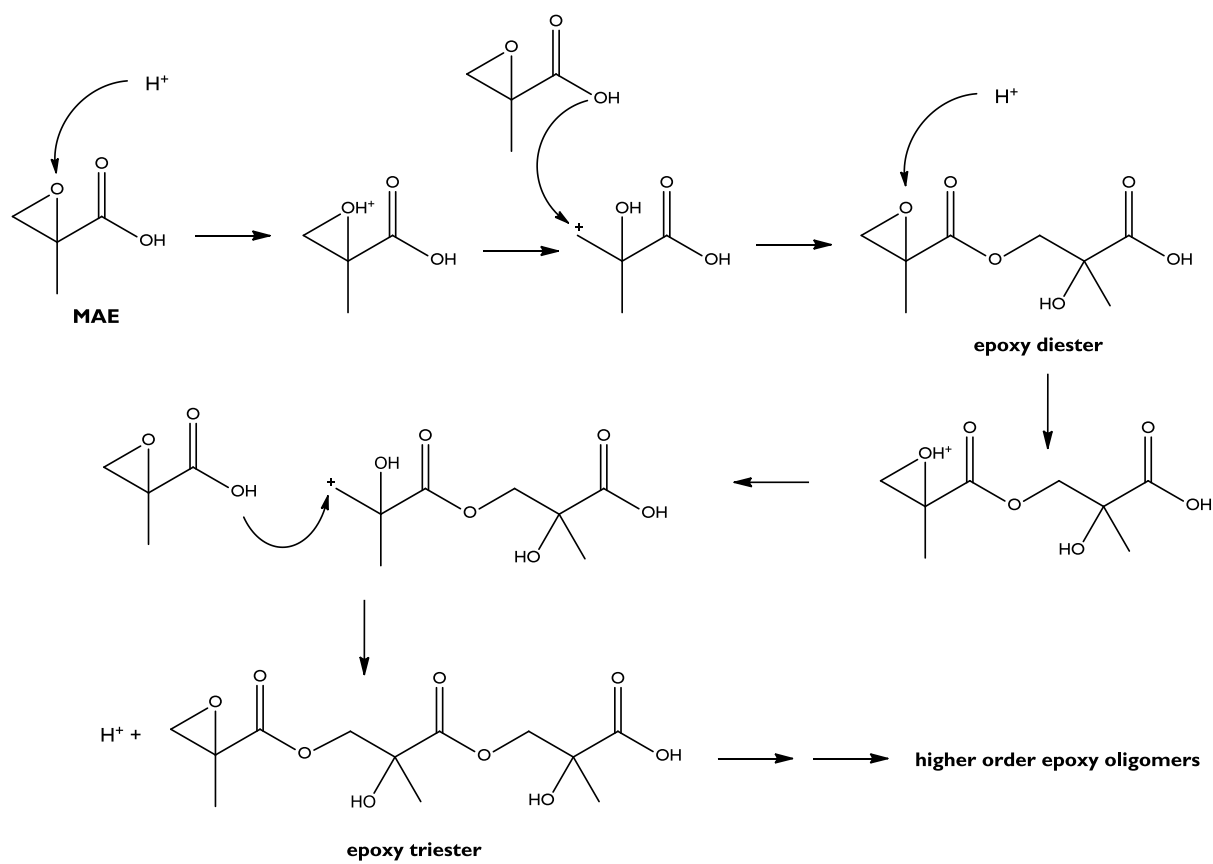
1
2
3

Fig. 4. Determination of acid-catalyzed MAE hydrolysis rate constant.



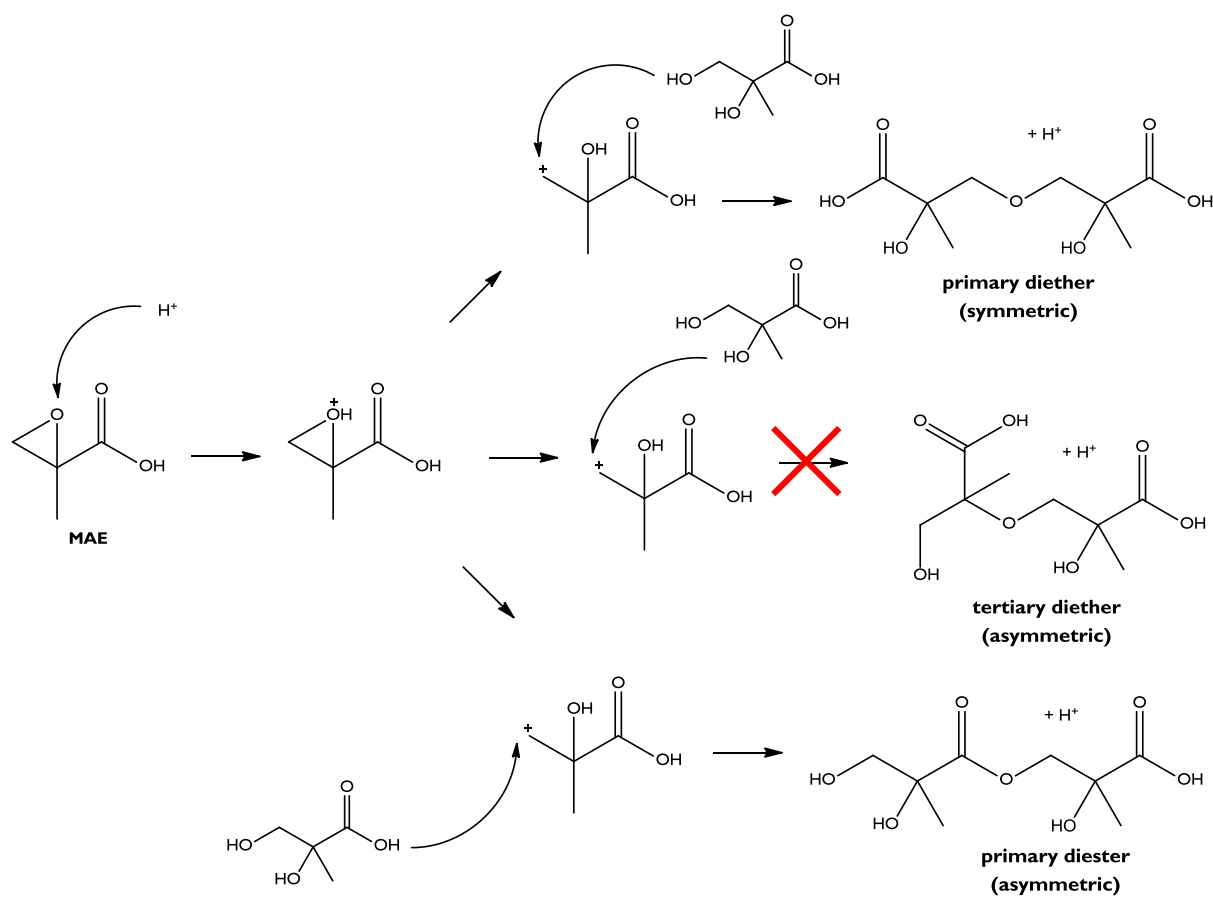
1
2
3
4
5

Fig. 5. Generalized MAE nucleophilic addition mechanism (the tertiary addition product was not observed for any MAE + nucleophile reactions).



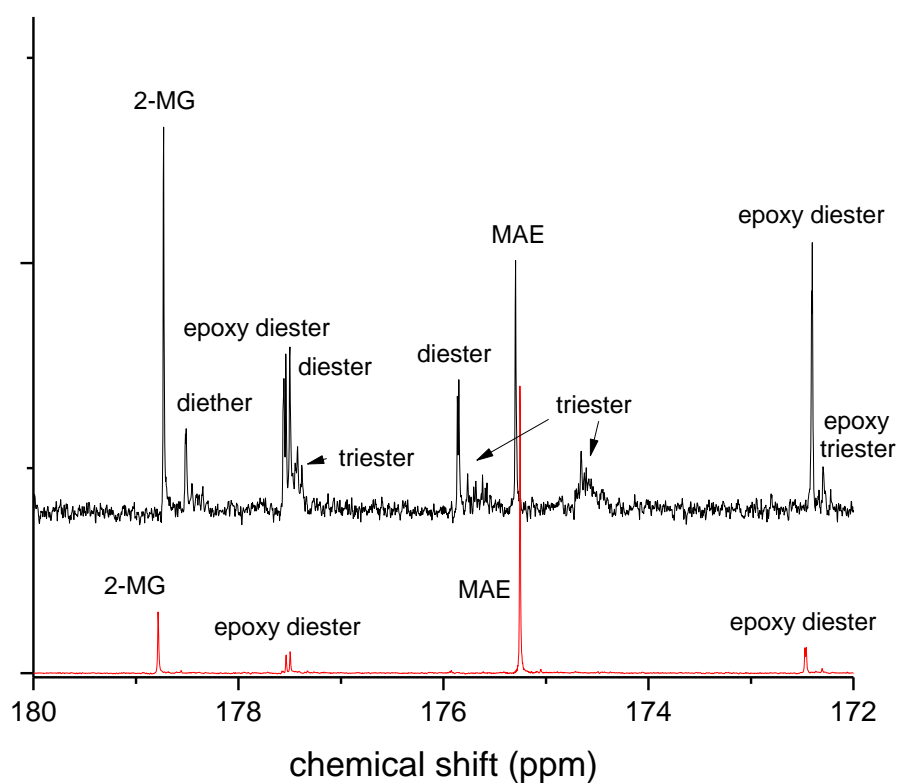
1
2
3

Fig. 6. MAE oligomerization (via epoxy chain reaction) mechanism.

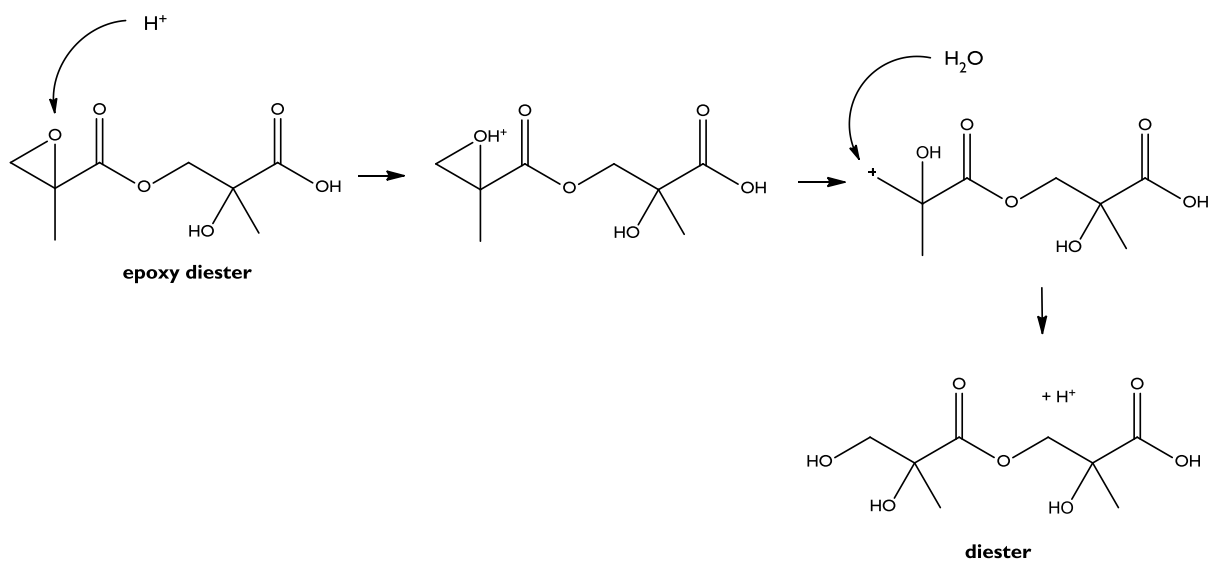


1
2
3
4

Fig. 7. Specific MAE + 2-MG nucleophilic addition mechanisms (the tertiary alcoholic OH group on 2-MG was not observed to participate in nucleophilic addition reactions).



1
 2
 3 **Fig. 8.** Carbonyl region ¹³C NMR spectra of early reaction (red trace) and late reaction (black
 4 trace) for experiment #4. See Figure 1 for the molecular species that correspond to the NMR
 5 peak labels.



1
2
3 **Fig. 9.** Epoxy diester hydrolysis mechanism.